Mansoura Engineering Journal

Volume 47 | Issue 6 Article 3

12-1-2022

Evaluation of Energy Detection-Based Spectrum Sensing for Cognitive Radio Applications

Rania. A. Youssef
Researcher of Electronics and Communications Engineering Department, Mansoura University, Mansoura, Egypt, raniausif@std.mans.edu.eg

Mohamed. A. Mohamed
Professor at the Electronics and Communications Engineering Department, Mansoura University, Mansoura, Egypt, mazim12@gmail.com

Ahmed A. Kabeel
Assistant Professor at the Electronics and Communications Engineering Department, Higher institute of engineering and Technology in New Damietta, New Damietta, Egypt, ahmede_kabeel@hotmail.com

Mansoura University
Faculty of Engineering
Mansoura Engineering Journal

Evaluation of Energy Detection-Based Spectrum Sensing for Cognitive Radio Applications

Rania. A. Youssef*, M. A. Mohamed and A. Kabeel

KEYWORDS:
microstrip antenna, Ultra-wide band, tunable antenna, cognitive radio, spectrum sensing, Energy Detector

Abstract— In this paper, a novel design of cognitive radio (CR) system based on a tunable ultra wide-band antenna is suggested; it offers a quick and cheap method for effectively locating spectrum gaps spanning. The frequency ranges of 9.30 to 13 GHz with three operating bandwidths (BW) of 1.11GHz ,0.8 GHz, and 0.36GHz. Frequency is scanned by using a tunable Ultra-Wideband, the antenna has a small size with five gaps that are used as a Switch 2 mm × 3 mm and the partial ground 30 mm × 30 mm, these Switches can offer a tuning capability. The suggested antenna is constructed on a Rogers RT5880 substrate with a relative permittivity (εr) =2.2 and a dielectric thickness of 1.575 mm. This design of antenna has a number of benefits, including small size, low cost, easy to fabricate, and band accessibility that is elastic, the ground and patch antenna are fabricated on copper. At 10 GHz, an overall realized gain of 8.65dBi is achieved. The low VSWR < 2 antenna presented has a suitable radiation characteristic to gratify the needs of existing and future wireless communication systems. Return loss simulation findings for different switch states and radiation patterns at different frequencies are also shown, at the end both simulation and measurements are presented.

I. INTRODUCTION

Wireless applications are developing quickly, so some frequency bands are busy, while others are infrequently used. Cognitive radio (CR) is thought to be a one-of-a-kind solution for bandwidth shortages that keeps balancing spectrum usage[1] . The most essential feature of the CR system is its awareness of the surrounding radio frequency (RF) environment. This is accomplished through the spectrum sensing, which is the constant observation of wireless channel activity [2]. The most difficult aspect of spectrum sensing is its practical application, which necessitates a reconfigurable forward future [3]. UWB system can be thought of as a gradation starting at close range. You might think of the employment of UWB systems as a gradation, starting with short-range communications and ending with security systems, ground- and object-penetrating radar, and other technologies, vehicle radar, and measurements applications. Their high data rate, large packaging for multi - path interference, and low power requirements for this [4]. The suggested antenna for UWB systems faces major challenges because to its wide frequency band coverage and handling of high-speed pulses. The antenna should respond extremely well to the UWB antennas designed applications described in [5] additional to having a high bandwidth, efficiency, and small size. You can communicate over a number of specified frequency bands by adjusting the ultra-wideband (UWB) sensor antenna. With the development of a number of applications

Received: (16 August, 2022) - Revised: (13 October, 2022) - Accepted: (17 October, 2022)

***Corresponding Author**: Rania. A. Youssef, Researcher at Electronics and Communications Engineering Department, Mansoura University, Mansoura, Egypt (e-mail: raniausif@std.mans.edu.eg).*

Mohamed. A. Mohamed, Professor at the Electronics and Communications Engineering Department, Mansoura University, Mansoura, Egypt (e-mail: Mazim12@gmail.com).

Ahmed. A. Kabeel, Lecturer at the Electronics and Communications Engineering Department, Higher institute of engineering and Technology in New Damietta, New Damietta, Egypt (e-mail: ahmede_kabeel@hotmail.com).

(Ser. NO. BFEMU-2207-1290)

requiring portable, short-range UWB antennas, the ability to reconfigure has been realized effectively. Some published research examined to operate in ultra-wideband antennas [6], [7]. We are based on an Energy detector, also known as radiometric, which is an extremely popular technique for spectrum applications (e.g., setting metal of copper to touch the gap of the patch as an ON switch state (1) and removing it for the OFF case (0)). Printed circuit board-based omnidirectional antennas are favored. Recently developments in this area have been reported in[8]–[12].

Because application complications and processing are not present, reconfiguring cognitive radios to use the same antenna for sensing and contact sensing[13]–[19]. It's also more popular (in comparison to other ways) because recipients don't need to know which information about the primary users. By contrasting the output of the energy detector with the threshold that counts on the noise floor, the signal is identified[20]. The threshold for detecting primary users of the energy detector has many sensory problems, such as inability to differentiate between interference principal users and noise, and poor performance during signal to noise ratio (SNR) reevaluation. [19]. The goal of this study is to design a microstrip patch antenna and Study how switching affects antenna parameters like gain, return loss, and VSWR, and radiation pattern. We have 32 different measurement scenarios because of the various switching configurations that have been presented in this research. CST Microwave Studio was used to perform out the simulation[21].

The remainder of the paper will be arranged as follows: in the second section, there is an Energy detector, antenna design is covered in the third section and section 4 is about manual tuning, simulated and measured results are discussed in section 5. Finally, the conclusions of section 6 and the paper's future work.

II. ENERGY DETECTOR

We used energy detection and the techniques of this system uses energy identification for spectrum sensing to determine the existence of primary users. This occurs when the received signal levels exceed a predetermined threshold λ; otherwise, the primary user signal is disabled. This method is simple to use and requires no prior awareness of PU. The probability of false alarm, the probability of detection, SNR, and the number of samples are all calculated using the energy detection method, which is written in MATLAB. The ratio of times the signal exceeds the threshold value and the total number of traces was evaluated to determine the probability of detection [22], and Due to its low processing and application measure of complication, this is the most ideal strategy for adjusting unknown signals when the noise is known. This is the most optimum technique to adjust the unknown signals when the noise is known due to it having low processing and application measure of complication.

A crucial phase of the cognitive radio cycle is spectrum sensing. It targets basically to choose between two states: primary user signal absence by *H0*, or primary user signal presence *H1*. These two states can be explained as (1), (2)

$H_0 : y(n) = w(n)$ (1) The signal is absent
$H_1 : y(n) = x(n) + w(n)$ (2) The signal is present

The received signal is represented by y(n), the transmitted signal is represented by x(n), and the noise affecting the transmitted signal is represented by w(n).

As shown in Fig. 1, the squared magnitude of the Fast Fourier Transform (FFT) of the received N samples, averaged across N samples, is used to determine the energy of these samples [20], [23], [24], using (3)

$$TED = \sum_{n=1}^{N} (Y[n])^2 \quad (3)$$

The energy *TED* is then contrasted to a pre-determined threshold λ_D to determine the sensing decision:

$TED > \lambda_D$: PU signal absence
$TED < \lambda_D$: PU signal presence

The probability of false alarm P_{FA} and The probability of detection P_d can be used to evaluate the algorithm's detection display. The probability of detection is calculated by dividing the number of true detections (PU present) by the total number of sensing experiences, whereas the probability of false alarm is calculated by dividing the number of times the PU is incorrectly detected by the total number of sensing experiences. The probabilities are as follows:

$$P_d = Pr(TED < \lambda_D; H_1) \quad (4)$$
$$P_{FA} = Pr(TED < \lambda_D; H_0) \quad (5)$$

λ_D is the sensing threshold, and *TED* works with the energy of N samples as defined by equation (3).Following [23], the probability of detection P_d and false alarm P_{FA} are is given by:

$$P_d = Q\left(\frac{\lambda - N(\sigma_W^2 + \sigma_x^2)}{(\sigma_W^2 + \sigma_x^2)\sqrt{2N}}\right) \quad (6)$$

$$P_{FA} = Q\left(\frac{\lambda_D - N\sigma_W^2}{\sigma_W^2\sqrt{2N}}\right) \quad (7)$$

Where *Q*-function $Q(x) = \frac{1}{2\pi}\int_x^\infty exp\left(\frac{-u^2}{2}\right) du$, σ_w, and σ_x are the standard eccentricity of the noise and the PU signal, and *N* is the number of samples, threshold λ_D, that is obtained (7) and served :

$$\lambda_D = \sigma_W^2 \left(Q^{-1}(P_{FA})\sqrt{2N} + N\right) \quad (8)$$

where $Q^{-1}(.)$ is the reverse of the Q-function.

The goal probability of a false alarm, the noise contrast, and the sample count are the basis for this threshold. Building an accurate threshold requires prior knowledge about the amount of noise that affects the received signal.

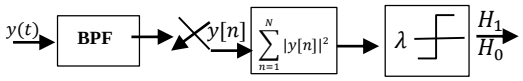

Fig. 1 block diagram of energy detector

For spectrum sensing, the probability of a false alarm should be low. To avoid the detector coming to the wrong conclusion, picks up the main signal H_1 rather than signal H_0. Because the detector lost the probability of detecting the free channel in this state, the secondary user would not use it.

A. Detection Performance Evaluation

Fig. 2 shows how MATLAB plots the probability of detection against the probability of false alarm. The simulated curve is based on one microstrip antenna element, M=1, small number of samples, *N*=1000, and a low signal-to-noise ratio, SNR= -20dB.

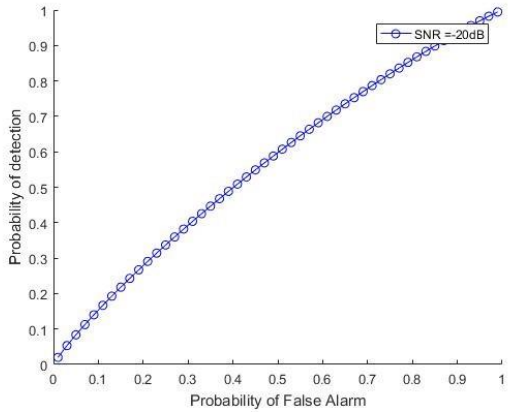

Fig. 2 the probability of detection P_d against the probability of false alarm P_{FA} curve are at proposed energy detector at M=1, *N*=1000 samples, and SNR= -20dB.

B. Noise Effect on Detection Performance

The exhibited energy detector's detection performance is rated, as well as the effect of white Gaussian noise, Fig. 3. shows the simulated probability of detection against SNR using MATLAB at M=1 element, *N*=1000 samples, and P_{FA} =0.1. It shows the highest performance, especially at SNR ($\geq -7\,dB$).

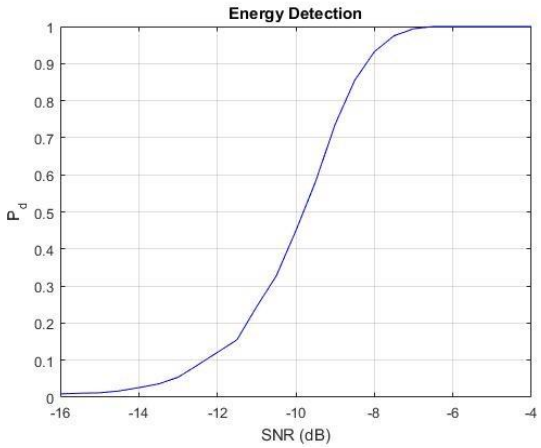

Fig. 3 The probability of detection against SNR for the proposed energy detector at M=1, *N*=1000 samples, and P_{FA} =0.1

C. Impact of Number of Samples on P_d

The number of received signal samples N is a very leading parameter to realize the detection requirements. Any increase in *N* will lead to perfection in detection performance. So, the probability of detection versus the number of samples is plotted using MATLAB as shown in Fig. 4 using *M*=1 element and P_{FA} =0.1 at SNR = -20 dB for *N*=3000, the P_d of the suggested energy detector reached the maximum value. Energy detectors exhibit high performance whatever *N* increases.

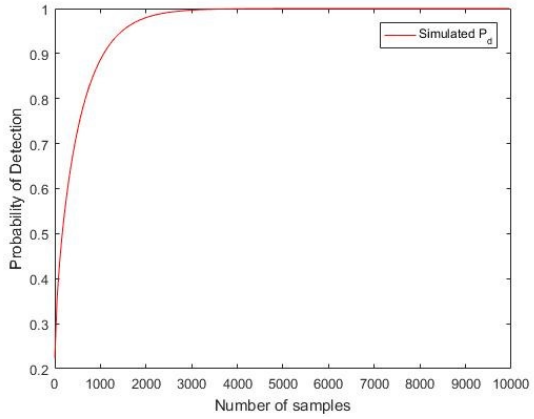

Fig. 4.The probability of detection against number of samples using M=1 and P_{FA} =0.1 at SNR = -20 dB

III. IMPACT OF ANTENNA ARRAY

A uniform linear array (ULA) with similar antenna elements is used in the case of antenna array, elements are uniformly distributed apart by an alignment of ($\Delta = \lambda/2$) where λ represents the signal's wavelength as it is being received.is the wavelength of the signal being received. The ULA is made to pick up signals received in narrowband by primary users. The antenna array's received signal is provided by:

$$y(n) = Ax(n) + w(n) \quad n=1, 2,..,N \tag{9}$$

where

$$y(n) = [y_1(n)y_2(n) \dots y_M(n)]^T \tag{10}$$
$$x(n) = [x_1(n)x_2(n) \dots x_d(n)]^T \tag{11}$$
$$w(n) = [w_1(n)w_2(n) \dots w_M(n)]^T \tag{12}$$

Where $x(n)$ and $w(n)$ are the vectors of the signal and noise columns, respectively. Complex white Gaussian noise (CWGN) with a zero mean is taken for granted as the noise type. The transposition operator is $[.]^T$. *A* is the $M \times d$ steering matrix can be written as

$$A = [\alpha(\mu_1)\alpha(\mu_2)..\alpha(\mu_d)] \tag{13}$$

Where $\alpha(\mu_1)$ is the steering vector which is given by

$$\alpha(\mu_i) = [e^{-j\mu i}\, e^{-j2\mu i} \dots e^{-j(M-1)\mu i}]^T \;, i = 1,2, \dots, d \tag{14}$$

Substituting equation (14) in equation (13), the steering matrix can be rewritten a

$$A = \begin{matrix} 1 & 1 & \dots & 1 \\ e^{-j\mu_1} & e^{-j\mu_2} & \dots & e^{-j\mu_d} \\ \vdots & \vdots & \ddots & \vdots \\ e^{-j(M-1)\mu_1} & e^{-j(M-1)\mu_2} & \dots & e^{-j(M-1)\mu_d} \end{matrix} \quad (15)$$

It depends on spatial frequencies $\mu_i = \frac{2\pi f_c}{c}\Delta sin\theta_i$, where the carrier frequency is f_c, c is the speed of light and θ_i is the direction of arrival (DOA). On the receiving end, it is assumed that the direction of arrival is known. The additional phase shifts caused by propagation delays from each element to the first reference point are represented as spatial frequencies.

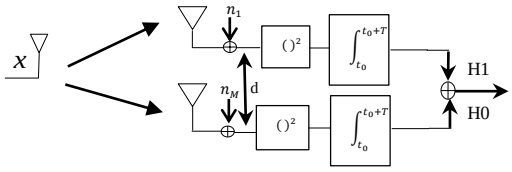

Fig. 5 block diagram of the proposed energy detector based on the antenna array

Fig 5 shows the block diagram of the proposed energy detector using a large number M of antennas. n_i is a variance-containing zero-mean circularly symmetric Gaussian variable σ_n^2, $d = \lambda/2$, the system uses time-division duplexing to function. We presume that every piece of equipment, whether it be an access point or user devices, has a large antenna array with each device using one antenna when transmitting and the entire array when receiving. It is assumed that the first component is at the starting point. The issue with binary hypothesis testing is now presented as

$H_0: y(n) = w(n)$ (16) signal absence

$H_1: y(n) = Ax(n) + w(n)$ (17) signal presence

When the noise variance is known, one of the most common detectors is the traditional energy detector using several antenna elements. It includes a test statistic provided by [25]

$$T_{ED(\sigma_w^2)}(y) = \frac{1}{MN\sigma_w^2}\sum_{m=1}^{M}\sum_{n=1}^{N}|y_m(n)|^2 \quad (18)$$

$$T_{ED(\sigma_w^2)} \begin{cases} > \lambda_{ED(\sigma_w^2)}, H_1 \\ < \lambda_{ED(\sigma_w^2)}, H_0 \end{cases} \quad (19)$$

Where $y_m(n)$ is the sampled signal received at m^{th} element and $\lambda_{ED(\sigma_w^2)}$ the decision threshold, When the variance of the noise is unknown, the estimated noise variance $\hat{\sigma}_w^2$ is used instead of σ_w^2 in (18). This estimate may not be correct and is subject to mistake [26]. This inaccuracy is additionally known as noise uncertainty α . The anticipated range for the estimated noise power is $[\frac{1}{\alpha}\sigma_w^2, \alpha\sigma_w^2]$ where $\alpha > 1$. Additionally, to achieve the appropriate false alarm probability under low SNR scenarios, a high number of samples are required. This issue is also known as SNR wall [27]. Table I displays an overview of the test statistics as well as the energy detection method's theoretical thresholds.

TABLE I
FORMULA FOR TEST STATISTICS AND THEORETICAL THRESHOLDS OF THE ENERGY DETECTOR

Method	Test statistic	Theoretical threshold
$ED(\sigma_w^2)$	$\frac{1}{MN\sigma_w^2}\sum_{m=1}^{M}\sum_{n=1}^{N}\|y_m(n)\|^2$	$2\Gamma_{inc}^{-1}(1-P_{FA}, MN)$
$ED(\hat{\sigma}_w^2)$	$\frac{1}{MN\hat{\sigma}_w^2}\sum_{m=1}^{M}\sum_{n=1}^{N}\|y_m(n)\|^2$	$Q_F^{-1}(1-P_{FA}, MN, L)$

Where Γi^{-1} is the inverse of the gamma function that is incomplete, Q^{-1} is the inverse of F-distribution function, and L is used as a smoothing factor.

A. *Detection Performance Evaluation*

One of the most popular Receiver Operating Characteristic (ROC) curves is provided in this case to evaluate the effectiveness of the energy detector. The ratio of the probability of detection $P_d$to the probability of a false alarm P_{FA} of the proposed energy detector are presented in Fig. 6 and Fig. 7 using small size ULAs consisting of M=2 elements up to M = 15 elements, N = 50 samples, and a low signal to noise ratio of SNR = -10dB.

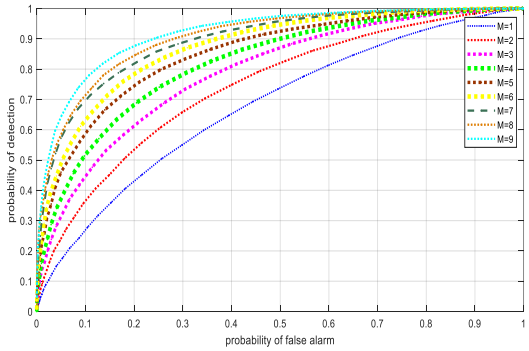

Fig. 6 Probability of detection P_d versus probability of false P_{FA} for energy detector using single antenna element M=1 and ULAs up to M=9 elements, N = 50 samples, and a low signal to noise ratio of SNR = -10 dB

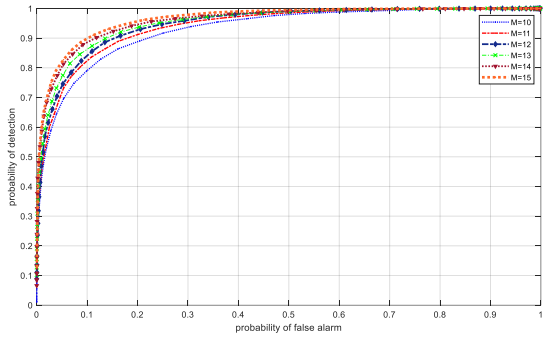

Fig. 7 Probability of detection P_d versus probability of false P_{FA} for energy detector using ULAs consisting of M=10 elements up to M=15 elements, N = 50 samples, and a low signal to noise ratio of SNR = -10 dB

B. *Noise Effect on Detection Performance Employing Different Number of Antenna Elements*

In this test case, the proposed energy detector's detection capabilities are evaluated in relation to the impact of AWGN. The simulated probability of detection P_d versus SNR at using single antenna element and ULAs consisting of M=2 elements

up to M = 10 elements, N = 100 samples, and P_{FA} = 0.1 is shown in Fig. 8. It offers the probability of detection across the entire SNR range $-25\ dB \leq SNR \leq 5\ dB$. It is clear that as the number of antenna elements increases, the probability of detection increases under the same noise effect.

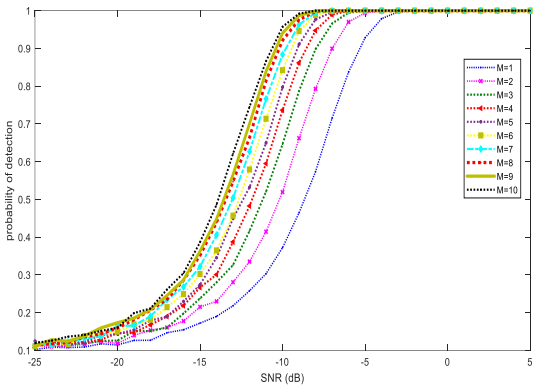

Fig. 8 Probability of detection P_d versus SNR at using single antenna element and ULAs consisting of M=2 elements up to M = 10 elements, N = 100 samples, and P_{FA} = 0.1.

C. Impact of Number of Samples On P_d

The received signal must be sampled N times in order to meet the detection requirements. Any increase in N should logically result in better detection performance. Fig. 9. Shows the probability of detection versus number of samples using M = 10 elements and P_{FA} = 0.1 at SNR = -20dB. It is clear that as the number of samples increases, the probability of detection increases under the same noise effect.

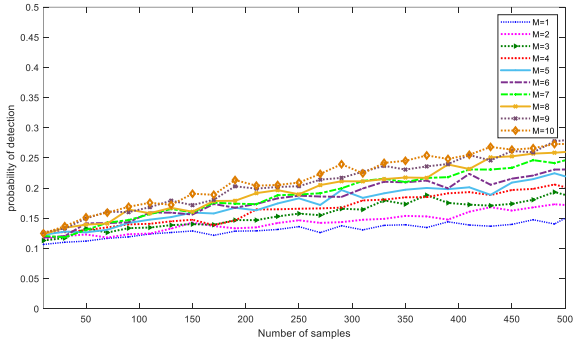

Fig. 9 Probability of detection versus number of samples N using M = 10 elements and P_{FA} = 0.1 at SNR =- 20dB.

IV. PROPOSED TUNABLE ANTENNA DESIGN

In this subsection, a microstrip patch antenna design for ultra-wideband applications is explained. Fig.10 shows the proposed UWB antenna element structure. This shape is utilized as it provides wide operating frequency band, and the proposed slots can be covered by a small copper to form a manual switch that changes the operating frequency of the antenna. Table II List the antenna's dimensions in millimetres (mm). The suggested antenna's predicted return loss $|S_{11}|$ against frequency is plotted in Fig. 11, which covers a large frequency range from 9.30 to 13 GHz. Below -10 dB for $|S_{11}|$ Fig. 12 showing Simulated $|S_{11}|$ parameter of the antenna element (Q9). The Ultra-wideband is used for the frequency scanning (UWB) using a manual switching technique that is described in the next section.

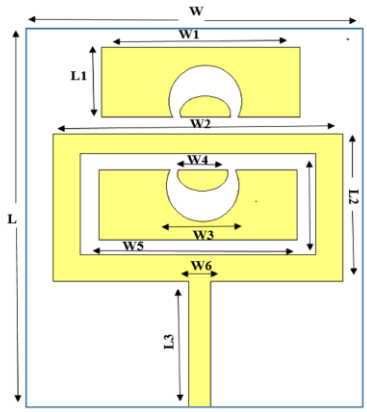

Fig. 10 Proposed UWB antenna element structure.

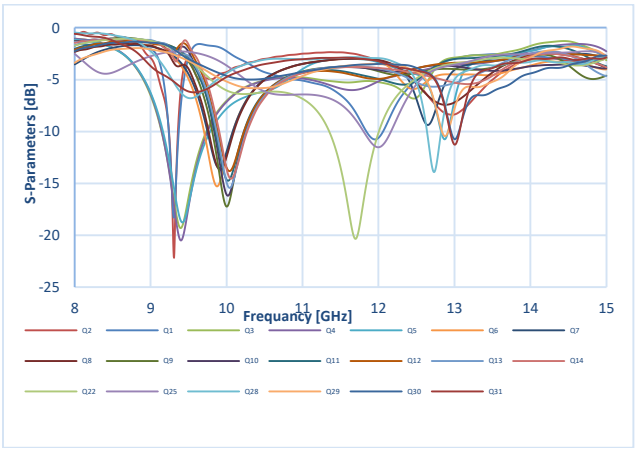

Fig 11. Simulated $|S_{11}|$ parameter ≤ -10dB.

TABLE II
DIMENSIONS OF THE PROPOSED UWB ANTENNA ELEMENT IN MM

Symbol	Value (in mm)	Symbol	Value (in mm)
W	30	W6	4
W1	16	L	30
W2	24	L1	5.5
W3	4	L2	13
W4	3.64	L3	8
W5	18	L4	9

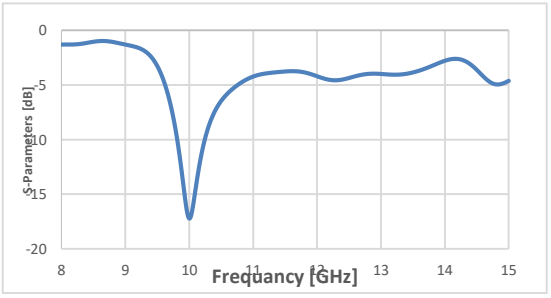

Fig. 12. Simulated $|S_{11}|$ parameter of the antenna element (Q9) without switch.

V. MANUAL TUNING

The antenna of a wireless system is crucial because it controls data transmission and reception at the physical layer. Numerous benefits can be derived from an antenna that has been properly tuned. It can increase a wireless device's effective range while consuming less power. In this design, we have five copper switching plates of dimensions (2 mm × 3 mm) of copper that we can place them manually in specific places, so we have the possibility of 32 tunning frequencies. Existence of a switch means (1) and the non-existence means (0). We named this probability (Q) and we have from Q1 to Q32. Table III lists the frequency , $|S_{11}|$ and the bandwidth. The antenna has a wide tunning range from 9.30 to 13 GHz. Using the gain comparison approach, the antenna gain is measured Fig. 13 shows the antenna gain for Q9, Q12.

VI. SIMULATED AND MEASURED RESULTS

Fig. 14 shows the fabricated microstrip antenna using a PCB different switching conditions. A small antenna was used to measure the radiation pattern, and Fig. 15 shows the $|S_{11}|$ parameter was measured using the ROHDE & SCHWARZ ZVB vector network analyzer. We have five witches to make the antenna more useful and meaningful, we got 20 frequencies in the range, and switches are placed such that they touch the antenna patch at the junction point, as indicated as indicated Table III frequency, $|S_{11}|$, and BW. Five switches put on a gap of 0.4 mm, includes a shift between them, allowing us to achieve several frequencies from a single design. The gain and VSWR are listed in Table IV

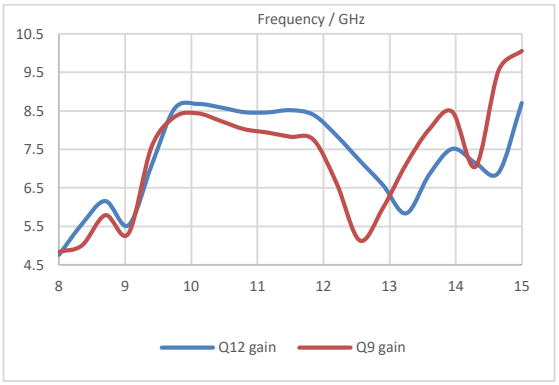

Fig 13 The antenna gain for Q9, Q12.

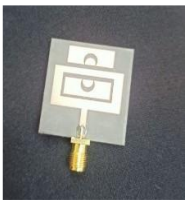

00000 (Q9)

00100 (Q3)

01110 (Q28)

01111 Q(22)

10010 (Q14)

Fig. 14 Fabricated microstrip antenna using a PCB at different switching conditions.

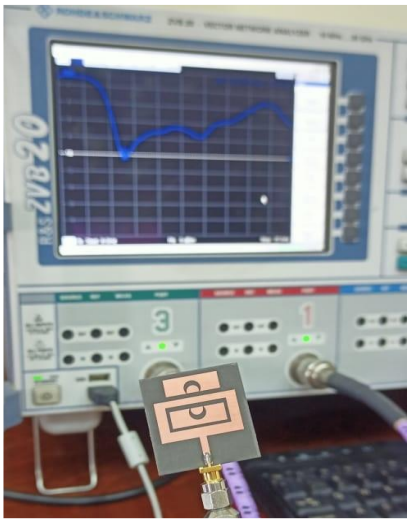

Fig. 15 $|S_{11}|$ measurement by using the ROHDE & SCHWARZ ZVB vector network analyser.

Fig. 16 explains the antenna's radiation. The antenna has excellent radiation characteristics and a gain of 8.65dBi at 10 GHz as shown in Fig 12 Q9 without switch and Q12 with three switches A, C, and D are ON and B, E is OFF . Over The y-z and x-y plane patterns can be noticed.

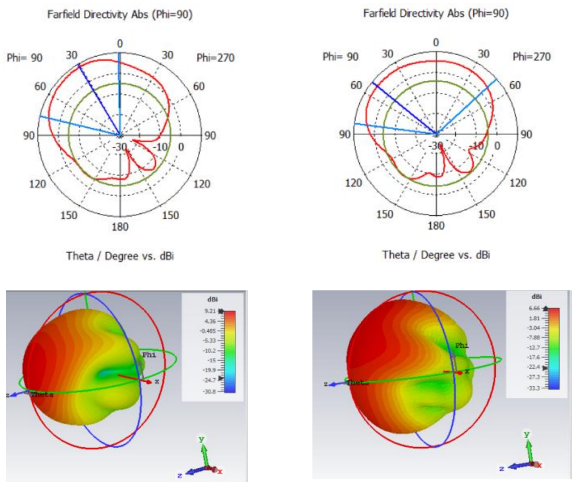

(a) (b)

Fig.16 radiation pattern (a) Q9 , (b) Q28

Also Fig. 17 depicts the comparison of simulated and measured $|S_{11}|$, where $|S_{11}|$ is less than -10dB. Furthermore, $|S_{11}|$ measurements are close to $|S_{11}|$ simulated , Table V lists the simulated and measured $|S_{11}|$ in different Q result's.

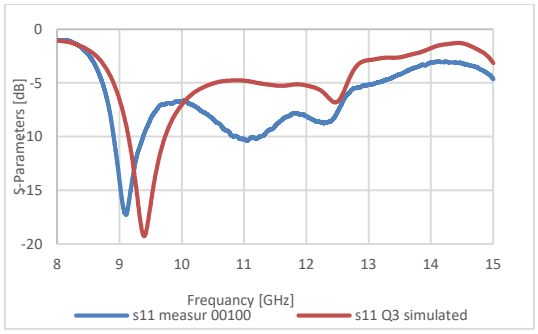

S11 Q(3)

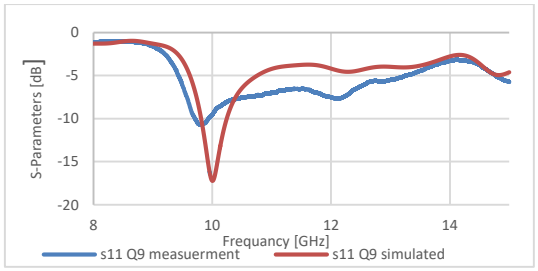

S11 Q(9)

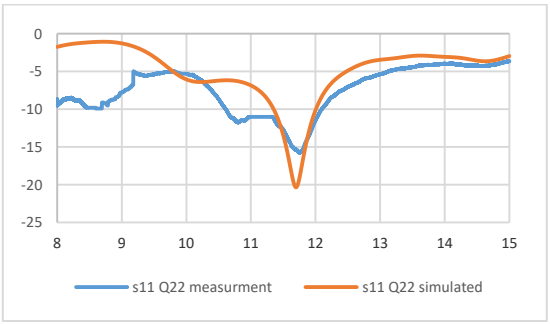

S11 Q(22)

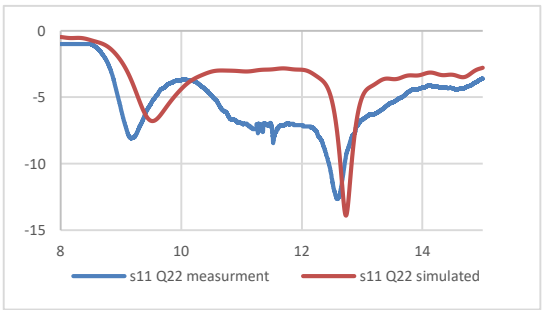

S11 Q (28)

Fig. 17 The *comparison of simulated and measured* $|S_{11}|$ *results.*

TABLE V
THE SIMULATED AND MEASURED $|S_{11}|$ IN DIFFERENT Q RESULT'S.

Q	Frequency(GHz)	$\|S_{11}\|$ (dB) simulated	$\|S_{11}\|$ (dB) measurement
Q3	9.39	-19.29	-17.41
Q9	10	-17.22	-10.6
Q22	11.7	-20.33	-15.38
Q28	12.73	-13.90	-11.99

The overall VSWR is improved by changing the switches and multiplicity frequency, as shown in Fig.18 the comparison of simulated and measured VSWR results, VSWR < 2 because of the smoother transmission from the feedline to the microstrip, as shown in Fig.18. Table VI lists the simulated and measured VSWR in different Q (Q3, Q9, Q22 and Q28) results.

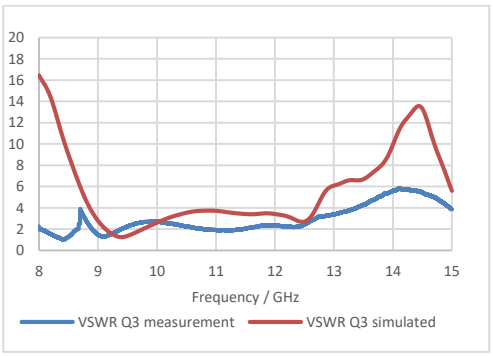

VSWR Q (3)

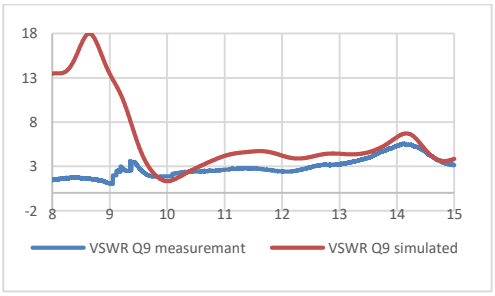

VSWR Q (9)

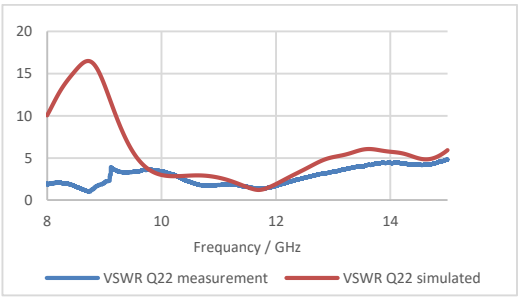

VSWR Q (22)

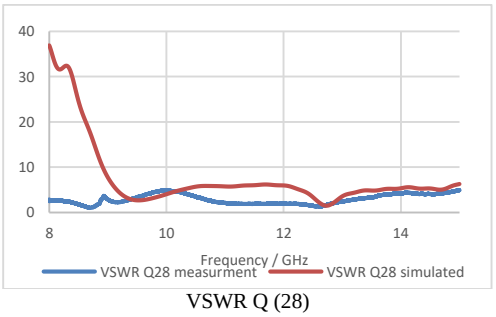

VSWR Q (28)

Fig. 18 The comparison of simulated and measured VSWR results

TABLE VI
THE SIMULATED AND MEASURED VSWR IN DIFFERENT Q RESULT'S.

Q	Frequency (GHz)	simulated	measured
Q3	9.39	1.29	1.31
Q9	10	1.31	1.83
Q22	11.7	1.21	1.39
Q28	12.73	1.5	1.35

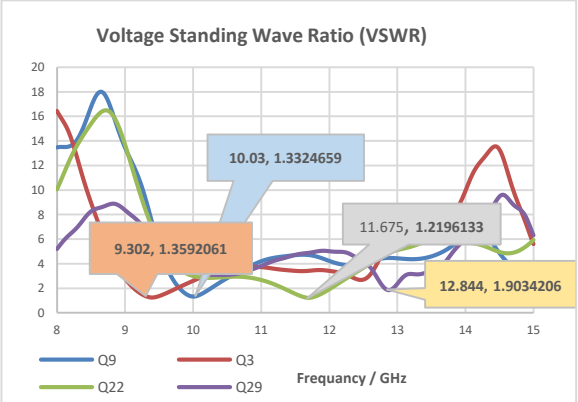

Fig 19 The simulated VSWR

Fig. 19 shows the simulated VSWR. Table VII contains a comparison of this work with related literary works. This comparison demonstrates that the suggested antenna has number of switches, number of bands, size of mm, and a substrate material. Fig. 20 shows the comparison between simulated and measured radiation patterns (normalized (a) Q9, (b) Q28).

TABLE VII
A COMPARISON OF THE SUGGESTED STRUCTURE AND RELATED LITERARY WORKS

References	No. of switch	No. of bands	Size (mm)	substrate
[28]	4	3	40×40	FR4
[29]	3	6	25×27	RO4350B
[30]	2	2	45×38	FR4
[31]	2	4	26×30	FR4
[32]	3	3	20×20	FR4
[33]	3	6	68.5×60	Taconic RF35
This work	**5**	**15**	**30×30**	**Rogers RT5880**

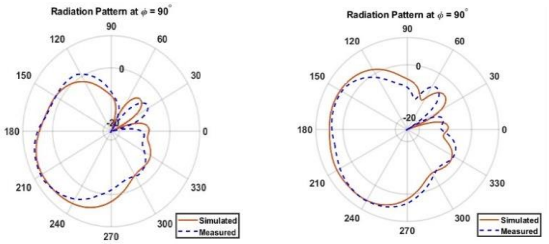

(a) (b)

Fig. 20 The comparison between simulated and measured radiation patterns (normalized (a) Q9, (b) Q28)

VII. CONCLUSION

This work proposes a novel design of a cognitive radio (CR) system based on a Tunable ultra-wideband antenna, which offers a quick and inexpensive method for effectively detecting spectrum holes in the frequency range from 9.30 to 13 GHz. High gain and radiation efficiencies of 8.65dBi and 80% are realized at 10 GHz. The antenna has excellent radiation characteristics and low VSWR < 2. In addition, simple and cheap materials were employed. The simulated and measured results show that the suggested CR system is more reliable and efficient.

APPENDIX

TABLE III
32 FREQUENCY Q1 TO Q32 (WHITE SELECTION IN THE RANGE, GRAY SELECTION OUT OF THE RANGE, ARRANGEMENT BASED ON THE FREQUENCY ASCENDING).

A	B	C	D	E	Q	frequency	$\lvert S_{11}\rvert$	B.W
0	1	0	1	1	Q1	9.30	-18.27	0.13
0	1	0	1	0	Q2	9.30	-22.16	0.12
0	0	1	0	0	Q3	9.39	-19.29	0.59
1	0	1	0	0	Q4	9.4	-20.49	0.60
1	1	1	0	0	Q5	9.42	-18.75	0.62
1	1	0	0	0	Q6	9.87	-15.28	0.38
1	1	1	1	0	Q7	9.90	-13.50	0.33
1	1	0	1	0	Q8	9.91	-13.67	0.33
0	0	0	0	0	Q9	10	-17.22	0.43
1	0	0	0	0	Q10	10.01	-16.18	0.41
0	0	1	1	0	Q11	10.02	-14.73	0.37
1	0	1	1	0	Q12	10.03	-13.81	0.34
0	0	0	1	0	Q13	10.04	-15.42	0.39
1	0	0	1	0	Q14	10.05	-14.54	0.37
0	0	0	0	1	Q15	10.54	-5.78	-
1	0	0	0	1	Q16	10.55	-5.60	-
0	0	1	1	1	Q17	10.91	-5.45	-
1	0	1	1	1	Q18	10.94	-5.17	-
0	0	0	1	1	Q19	11.06	-3.91	-
1	0	0	1	1	Q20	11.08	-3.65	-
0	0	1	0	1	Q21	11.5	-5.36	-
0	1	1	1	1	Q22	11.69	-20.33	0.65
1	0	1	0	1	Q23	11.72	-6.30	-
0	1	0	0	1	Q24	11.91	-6.83	-
1	1	1	1	1	Q25	11.99	-11.51	0.36
1	1	0	1	1	Q26	12.24	-5.38	-
0	1	0	0	0	Q27	12.37	-7.72	-
0	1	1	1	0	Q28	12.73	-13.90	0.18
1	1	1	0	1	Q29	12.87	-10.44	0.08
0	1	1	0	1	Q30	13.00	-10.74	0.1
0	1	1	0	0	Q31	13.00	-11.26	0.12
1	1	0	0	1	Q32	13.39	-5.78	-

TABLE IV
VSWR, GAIN (WHITE SELECTION IS IN THE RANGE, THE GREY SELECTION IS OUT OF THE RANGE).

A	B	C	D	E	Q	VSWR	Gain
0	1	0	1	1	Q1	1.27	5.84
0	1	0	1	0	Q2	1.16	5.46
0	0	1	0	0	Q3	1.24	8.3
1	0	1	0	0	Q4	1.20	8.46
1	1	1	0	0	Q5	1.26	8.27
1	1	0	0	0	Q6	1.41	7.76
1	1	1	1	0	Q7	1.53	7.73
1	1	0	1	0	Q8	1.52	7.67
0	0	0	0	0	Q9	1.31	8.40
1	0	0	0	0	Q10	1.36	8.53
0	0	1	1	0	Q11	1.44	8.49
1	0	1	1	0	Q12	1.51	8.65
0	0	0	1	0	Q13	1.40	8.46
1	0	0	1	0	Q14	1.46	8.61
0	0	0	0	1	Q15	3.21	5.45
1	0	0	0	1	Q16	3.20	5.46
0	0	1	1	1	Q17	3.28	5.65
1	0	1	1	1	Q18	3.45	5.75
0	0	0	1	1	Q19	4.51	5.81
1	0	0	1	1	Q20	4.81	5.92
0	0	1	0	1	Q21	3.34	8.12
0	1	1	1	1	Q22	1.21	8.15
1	0	1	0	1	Q23	2.87	8.02
0	1	0	0	1	Q24	2.66	7.08
1	1	1	1	1	Q25	1.72	7.25
1	1	0	1	1	Q26	3.23	6.59
0	1	0	0	0	Q27	2.39	5.28
0	1	1	1	0	Q28	1.5	5.59
1	1	1	0	1	Q29	1.85	4.9
0	1	1	0	1	Q30	1.81	5.65
0	1	1	0	0	Q31	1.75	5.04
1	1	0	0	1	Q32	3.11	6.97

AUTHORS CONTRIBUTION

Contribution	Authors
Conception or design of the work	***Ahmed. A. Kabeel***
Data collection and tools	***Rania. A. Youssef***
Data analysis and interpretation	***Rania. A. Youssef***
Funding acquisition	***No funding***
Investigation	***Rania. A. Youssef***
Methodology	***Ahmed. A. Kabeel***
Project administration	***Mohamed. A. Mohamed***
Resources	***Rania. A. Youssef,***
Software	***Rania. A. Youssef***
Supervision	***Mohamed. A. Mohamed***
Drafting the article	***Rania. A. Youssef***
Critical revision of the article	***Mohamed. A. Mohamed***
Final approval of the version to be published	***Mohamed. A. Mohamed***

FUNDING STATEMENT:

The author did not receive any financial support of the research authorship and publication of this article.

DECLARATION OF CONFLICTING INTERESTS STATEMENT:

The author declared that there are no potential conflicts of interest with respect to the research authorship or publication of this article.

REFERENCES

[1] J. Walko, "Cognitive radio," *IEE Rev.*, vol. 51, no. 5, pp. 34–37, 2005, doi: 10.1049/ir:20050504.

[2] T. Aboufoul, A. Alomainy, and C. Parini, "Reconfiguring UWB monopole antenna for cognitive radio applications using GaAs FET switches," *IEEE Antennas Wirel. Propag. Lett.*, vol. 11, pp. 392–394, 2012, doi: 10.1109/LAWP.2012.2193551.

[3] F. F. Digham, M. S. Alouini, and M. K. Simon, "On the energy detection of unknown signals over fading channels," *IEEE Trans. Commun.*, vol. 55, no. 1, pp. 21–24, 2007, doi: 10.1109/TCOMM.2006.887483.

[4] M. Gopikrishna, D. D. Krishna, A. R. Chandran, and C. K. Aanandan, "Square monopole antenna for ultra wide band communication applications," *J. Electromagn. Waves Appl.*, vol. 21, no. 11, pp. 1525–1537, 2007, doi: 10.1163/156939307782000299.

[5] I. Oppermann, M. Hamalainen, and J. Iinatti, *UWB: Theory and applications*. 2005.

[6] T. Aboufoul and A. Alomainy, "Reconfigurable printed UWB circular disc monopole antenna," *LAPC 2011 - 2011 Loughbrgh. Antennas Propag. Conf.*, no. November, pp. 15–18, 2011, doi: 10.1109/LAPC.2011.6114078.

[7] Q. Mary and M. E. Road, "Sing le-Elem ment Re econfig urable Planar r Ultra Wideba Ante enna fo or Cogn nitive Radio Fr ront En nd," pp. 0–4, 2011.

[8] S. Y. Chen, P. H. Wang, and P. Hsu, "Uniplanar log-periodic slot antenna fed by a CPW for UWB applications," *IEEE Antennas Wirel. Propag. Lett.*, vol. 5, no. 1, pp. 256–259, 2006, doi: 10.1109/LAWP.2006.873956.

[9] S. W. Qu, J. L. Li, and Q. Xue, "A band-notched ultrawideband printed monopole antenna," *IEEE Antennas Wirel. Propag. Lett.*, vol. 5, no. 1, pp. 495–498, 2006, doi: 10.1109/LAWP.2006.886303.

[10] A. A. Eldek, A. Z. Elsherbeni, and C. E. Smith, "Rectangular slot antenna with patch stub for ultra wideband applications and phased array systems," *Prog. Electromagn. Res.*, vol. 53, pp. 227–237, 2005, doi: 10.2528/PIER04092701.

[11] A. A. Eldek, "Numerical analysis of a small ultra wideband microstrip-fed tap monopole antenna," *Prog. Electromagn. Res.*, vol. 65, pp. 59–69, 2006, doi: 10.2528/PIER06082305.

[12] S. Sadat, S. D. S. Javan, and M. Houshmand, "Design of a microstrip square-ring slot antenna filled by an H-shape slot for UWB applications," *IEEE Antennas Propag. Soc. AP-S Int. Symp.*, no. July, pp. 705–708, 2007, doi: 10.1109/APS.2007.4395591.

[13] A. Annamalai and A. Olaluwe, "On the energy detection of unknown signals in κ-μ And η-μ fading channels with diversity receivers," *2013 Int. Conf. Connect. Veh. Expo, ICCVE 2013 - Proc.*, pp. 127–132, 2013, doi: 10.1109/ICCVE.2013.6799781.

[14] N. Sai Shankar, C. Cordeiro, and K. Challapali, "Spectrum agile radios: Utilization and sensing architectures," *2005 1st IEEE Int. Symp. New Front. Dyn. Spectr. Access Networks, DySPAN 2005*, pp. 160–169, 2005, doi: 10.1109/DYSPAN.2005.1542631.

[15] P. Pawełczak, G. J. M. Janssen, and R. V. Prasad, "Performance measures of dynamic spectrum access networks," *GLOBECOM - IEEE Glob. Telecommun. Conf.*, 2006, doi: 10.1109/GLOCOM.2006.671.

[16] P. Qihang, Z. Kun, W. Jun, L. Shaoqian, and S. Province, "and Evidence Theory in Cognitive Radio Context," *Sci. Technol.*, 2006.

[17] Y. Yuan *et al.*, "Knows: Cognitive radio networks over white spaces," *2007 2nd IEEE Int. Symp. New Front. Dyn. Spectr. Access Networks*, pp. 416–427, 2007, doi: 10.1109/DYSPAN.2007.61.

[18] A. Ghasemi and E. S. Sousa, "Optimization of spectrum sensing for opportunistic spectrum access in cognitive radio networks," *2007 4th*

Annu. IEEE Consum. Commun. Netw. Conf. CCNC 2007, pp. 1022–1026, 2007, doi: 10.1109/CCNC.2007.206.

[19] H. Tang, "Some physical layer issues of wide-band cognitive radio systems," *2005 1st IEEE Int. Symp. New Front. Dyn. Spectr. Access Networks, DySPAN 2005*, pp. 151–159, 2005, doi: 10.1109/DYSPAN.2005.1542630.

[20] A. Ranjan, Anurag, and B. Singh, "Design and analysis of spectrum sensing in cognitive radio based on energy detection," *2016 Int. Conf. Signal Inf. Process. IConSIP 2016*, no. February, pp. 3–7, 2017, doi: 10.1109/ICONSIP.2016.7857444.

[21] R. Ahmed, M. A. Mohammed, and A. A. Kabeel, "Characterization of tunable Ultra-Wideband Square Microstrip antenna with several gaps," *Int. Telecommun. Conf. ITC-Egypt 2022 - Proc.*, 2022, doi: 10.1109/ITC-Egypt55520.2022.9855686.

[22] Y. Zhao, S. Li, N. Zhao, and Z. Wu, "A novel energy detection algorithm for spectrum sensing in cognitive radio," *Inf. Technol. J.*, vol. 9, no. 8, pp. 1659–1664, 2010, doi: 10.3923/itj.2010.1659.1664.

[23] M. R. Manesh, M. S. Apu, N. Kaabouch, and W. C. Hu, "Performance evaluation of spectrum sensing techniques for cognitive radio systems," *2016 IEEE 7th Annu. Ubiquitous Comput. Electron. Mob. Commun. Conf. UEMCON 2016*, 2016, doi: 10.1109/UEMCON.2016.7777829.

[24] R. T. Khan, M. I. Islam, S. Zaman, and M. R. Amin, "Comparison of cyclostationary and energy detection in cognitive radio network," *IWCI 2016 - 2016 Int. Work. Comput. Intell.*, no. December, pp. 165–168, 2017, doi: 10.1109/IWCI.2016.7860359.

[25] A. Mariani, A. Giorgetti, and M. Chiani, "Effects of noise power estimation on energy detection for cognitive radio applications," *IEEE Trans. Commun.*, vol. 59, no. 12, pp. 3410–3420, 2011, doi: 10.1109/TCOMM.2011.102011.100708.

[26] Q. T. Zhang, "Advanced detection techniques for cognitive radio," *IEEE Int. Conf. Commun.*, no. 1, 2009, doi: 10.1109/ICC.2009.5198712.

[27] R. Tandra and A. Sahai, "SNR walls for signal detection," *IEEE J. Sel. Top. Signal Process.*, vol. 2, no. 1, pp. 4–17, 2008, doi: 10.1109/JSTSP.2007.914879.

[28] H. Boudaghi, M. Azarmanesh, and M. Mehranpour, "A frequency-reconfigurable monopole antenna using switchable slotted ground structure," *IEEE Antennas Wirel. Propag. Lett.*, vol. 11, pp. 655–658, 2012, doi: 10.1109/LAWP.2012.2204030.

[29] L. Han, C. Wang, X. Chen, and W. Zhang, "Compact Frequency-Reconfigurable Slot Antenna for Wireless Applications," *IEEE Antennas Wirel. Propag. Lett.*, vol. 15, no. c, pp. 1795–1798, 2016, doi: 10.1109/LAWP.2016.2536778.

[30] I. Bulu and H. Caglayan, "Designing Materials With Desired," *Microw. Opt.*, vol. 48, no. 12, pp. 2611–2615, 2006, doi: 10.1002/mop.

[31] D. Thiripurasundari and D. S. Emmanuel, "Switchable ultra wideband antenna for indoor and automotive vehicular band applications," *Int. J. Microw. Opt. Technol.*, vol. 8, no. 1, pp. 1–5, 2013.

[32] M. Borhani, P. Rezaei, and A. Valizade, "Design of a Reconfigurable Miniaturized Microstrip Antenna for Switchable Multiband Systems," *IEEE Antennas Wirel. Propag. Lett.*, vol. 15, no. c, pp. 822–825, 2016, doi: 10.1109/LAWP.2015.2476363.

[33] L. Han, L. Guo, R. Ma, and W. Zhang, "Frequency reconfigurable microstrip patch antenna," *WIT Trans. Inf. Commun. Technol.*, vol. 49, no. APACE, pp. 423–430, 2014, doi: 10.2495/ICIE130491.

Title Arabic:

تقييم استشعار الطيف المعتمد على اكتشاف الطاقة لتطبيقات الراديو الإدراكية

Arabic Abstract:

تم اقتراح تصميم جديد لنظام الراديو المعرفي(CR)على أساس هوائي واسع النطاق قابل للضبط في هذا البحث ، والذي يوفر حلاً سريعًا ومنخفض التكلفة للكشف الفعال عن ثقوب الطيف في نطاق التردد من ٩,٣٠ إلى ١٣ جيجا هرتز. يتم تحقيق كفاءات عالية في الكسب والإشعاع تبلغ ٨,٦٥ ديسيبل و ٨٠ ٪ عند ١٠ جيجاهرتز. يتميز الهوائي بخصائص إشعاعية ممتازة وانخفاض VSWR <2. علاوة على ذلك ، تم استخدام مواد بسيطة وغير مكلفة. يعتبر نظام CR المقترح أكثر كفاءة ودقة، وفقًا لنتائج المحاكاة والقياس.